Vehicular Communications 41 (2023) 100601

Contents lists available at ScienceDirect

Vehicular Communications

journal homepage: www.elsevier.com/locate/vehcom

ADOPT: A system for Alerting Drivers to Occluded Pedestrian Traffic ☆

Abrar Alali [a,b,*], Stephan Olariu [a], Shubham Jain [c]

[a] Old Dominion University, 5115 Hampton Blvd, Norfolk, 23529, VA, USA
[b] Saudi Electronic University, 4552 Prince Mohammed Ibn Salman Ibn Abdulaziz Rd, Riyadh, 13316, Saudi Arabia
[c] Stony Brook University, 100 Nicolls Rd, Stony Brook, 11794, NY, USA

ARTICLE INFO

Article history:
Received 1 October 2022
Received in revised form 24 January 2023
Accepted 10 March 2023
Available online 15 March 2023

Keywords:
Vehicle-to-Vehicle communications
Vehicle-to-Pedestrian communications
Pedestrian safety
Driver assistance

ABSTRACT

Recent statistics reveal an alarming increase in accidents involving pedestrians (especially children) crossing the street. A common philosophy of existing pedestrian detection approaches is that this task should be undertaken by the moving cars[1] themselves. In sharp departure from this philosophy, we propose to enlist the help of cars parked along the sidewalk to detect and protect crossing pedestrians. In support of this goal, we propose ADOPT: a system for Alerting Drivers to Occluded Pedestrian Traffic. ADOPT lays the theoretical foundations of a system that uses parked cars to: (1) detect the presence of a group of crossing pedestrians – a crossing cohort; (2) predict the time the last member of the cohort takes to clear the street; (3) send alert messages to those approaching cars that may reach the crossing area while pedestrians are still in the street; and, (4) show how approaching cars can adjust their speed, given several simultaneous crossing locations. Importantly, in ADOPT all communications occur over very short distances and at very low power. Our extensive simulations using SUMO-generated pedestrian and car traffic have shown the effectiveness of ADOPT in detecting and protecting crossing pedestrians.

1. Introduction and motivation

According to the National Highway Traffic Safety Administration, 6,301 pedestrians were hit and killed by drivers in the first half of 2021, a 17% increase over 2020[2] [1]. Recent studies [2,3] concluded that one of the main causes of crashes involving pedestrians is occlusion: the driver is unaware of the presence of pedestrians because some object partially or fully occludes them. Therefore, detecting occluded pedestrians reliably and in a timely manner is key to promoting pedestrian safety [4].

A glance at the recent literature reveals an increasing number of publications that leverage the on-board sensing and communication capabilities of present-day cars to increase the drivers' awareness of surrounding pedestrians. On-board cameras, short- and long-range laser devices, and Light Detection and Ranging (LiDAR) are part of the arsenal of sensors employed to detect pedestrians [5]. One common characteristic of these sensors is that they require Line-of-Sight (LoS) to enable detection [6]. Because of this, partially or totally occluded pedestrians go undetected most of the time [7]. In addition to the LoS challenge, weather and lighting conditions (e.g., glinting sun or other reduced visibility conditions) are apt to thwart the ability of on-board sensors to detect pedestrians [8,9].

One approach for detecting pedestrians that does not require LoS involves leveraging wireless communication technologies such as WiFi, Dedicated Short Range Communication (DSRC), Zigbee or Bluetooth. While this approach mitigates the LoS challenge, it has serious scalability problems. Indeed, reporting pedestrians within a large radio coverage area tends to be unreliable due to known impairments of radio transmission, various forms of interference, message propagation delays, and security concerns [10].

Recently, a number of researchers have suggested supplementing the data collected by on-board sensors with information collected by pre-deployed roadside infrastructure [11]. Aligned with this idea, several projects have been implemented at signalized intersections to promote pedestrian safety [12]. These projects involve installing sensors, cameras, and communication units in roadside infrastructure, such as light poles, to detect pedestrians and to alert approaching cars [13]. Although this approach enables the detection of occluded pedestrians, it focuses on signalized intersections, while the majority of pedestrian accidents tend to occur mid-block [14–16]. Moreover, this approach is problematic since roadside infrastructure may not be available when needed [9].

☆ Research funded by the NSF grant CNS-1951789 and CNS-2106594.
* Corresponding author.
E-mail addresses: aalal003@odu.edu, a.alali@seu.edu.sa (A. Alali), olariu@cs.odu.edu (S. Olariu), jain@cs.stonybrook.edu (S. Jain).
[1] In this work we refer to vehicles simply as cars.
[2] The report accounted for the effects of COVID-19 pandemic.

https://doi.org/10.1016/j.vehcom.2023.100601
2214-2096/

Recently, the potential of using parked vehicles as alternative road-side infrastructure in support of sensing and networking has been recognized by a number of researchers. For example, [17] and [18] suggested that the parked cars can be used as relying nodes in the network when they retransmit the received messages to the incoming cars to enhance the connectivity in VANET.

More recently, it was suggested to aggregate information collected by several moving vehicles in an effort to enable a *collaborative perception* of surrounding pedestrians [8]. The idea is that when a moving vehicle has a LoS connection to a group of pedestrians, it alerts neighboring vehicles, making them aware of the presence of potentially occluded pedestrians. Alternatively, using Vehicle-to-Pedestrian (V2P) communications [11], the pedestrians are alerted to the presence of approaching cars by pushing messages to their hand-held or wearable devices. Collaborative perception is a promising technology for enhancing pedestrian safety. However, in order to work effectively, the collaborative pedestrian detection methodology requires sophisticated sensing resources and communication protocols and may not scale well to a large number of pedestrians [19]. Furthermore, it is rather inaccurate since it relies on inaccurate GPS coordinates to estimate the distance between the pedestrian detected and the vehicle, not to mention the potentially high power consumption [20]. Most importantly, the alert messages sent via DSRC can easily overwhelm the network with unnecessary alerts [21].

1.1. Our contributions

The underlying design philosophy of all the approaches mentioned above is that pedestrian detection is to be undertaken by *moving cars* with all the complications that this entails. In sharp departure from this philosophy, we propose *ADOPT: a system for Alerting Drivers to Occluded Pedestrian Traffic* that runs on cars *parked* along the sidewalk.

By design, ADOPT is a low-power system whose stated goal is to alert approaching vehicles to the presence of possibly occluded pedestrians in the street. To implement this functionality, in ADOPT, all communications occur over very short distances and at very low power. Piezo-electric cells implanted in pedestrians' shoes power rudimentary radio transmitters that operate by closing a circuit as the pedestrian's shoes touch the ground. The resulting signals (essentially, radio noise) allow low-power transceivers, installed close to the four corners of parked cars, and integrated into the Controller Area Network (CAN) intra-vehicle network [22], to classify pedestrians as *on the sidewalk* or *in the street*. As long as the pedestrians stay on the sidewalk, ADOPT remains in a low-power vigilant state. When one or several pedestrians step into the street, ADOPT wakes up, locates the crossing pedestrians (a.k.a. crossing cohort), and estimates the time it takes the last member of the cohort to cross the street. By multi-hopping this information through a chain of parked cars along the sidewalk, ADOPT shares with the drivers of approaching cars (a) the location, on a digital map, of the crossing cohort ahead of them; and, (b) the estimated time it takes the cohort to cross the street.

To summarize, the main contributions of ADOPT are related to pedestrian safety and driver assistance. Specifically, this paper:

1. provides the theoretical foundations of a low-power and infrastructure-free occluded pedestrian detection system;
2. introduces a novel criterion for the *binary* classification of pedestrians as "on the sidewalk" or "in the street";
3. offers a scheme for estimating the expected time it takes the crossing cohort to clear the street;
4. provides an algorithm that allows approaching cars to adjust dynamically their speed, given several simultaneous crossing locations.

The remainder of this work is structured as follows: Section 2 offers a succinct survey of relevant recent work. Section 3 establishes terminology and discusses system assumptions. A detailed discussion of how ADOPT works can be found in Sections 4–7. Specifically, Section 4 offer the details of pedestrian classification and localization. Section 5 offers the details of the way ADOPT estimates the time it takes a cohort to cross the street. Next, Section 6 discusses the details of propagating alert messages to inform approaching cars of the presence of crossing pedestrians. In Section 7 we present an algorithm that can be used by approaching cars to adjust their speed as a result of receiving information about one or several crossing cohorts. The simulation models and the evaluation results of ADOPT are presented in Section 8. Finally, Section 9 offers concluding remarks and maps out directions for future investigations.

2. Relevant related work

The main goal of this section is to offer a succinct overview of the latest pedestrian detection systems and relevant emerging technologies.

2.1. On-board LoS sensors

The literature on pedestrian detection by vehicle's LoS on-board sensors such as various camera technologies, LiDAR, and Laser is quiet vast. LoS on-board sensors can detect pedestrians directly if they fully appear in the view. In [23], on-board infrared camera has been used to detect pedestrian on street. Laser has been also fused with the camera to detect pedestrians and calculate their speed in [24] while [25] fused thermal sensors with the stereo camera to detect pedestrians in low-visibility conditions.

However, if pedestrians are partially occluded, additional effort is needed to recognize them by on-board camera utilizing deep learning and convolutional networks [26–29]. In addition, sensor fusion approaches have been leveraged to detect partially occluded pedestrians. Recently, [30] used on-board thermal infrared sensors to detect pedestrians partially occluded by parked cars. [31] suggested fusing on-board LiDAR and radar to detect pedestrians partially occluded by. While on-board LoS sensors can detect partially occluded pedestrians, fully occluded pedestrians cannot be detected using the same sensors. Furthermore, relying on LoS sensors for occluded pedestrian detection must involve extensive vision algorithms that may not perform the task in a timely manner.

While on-board LoS sensors can detect partially occluded pedestrians, fully occluded pedestrians cannot be detected using the same sensors. Furthermore, relying on LoS sensors for occluded pedestrian detection must involve complicated computer vision algorithms that may not perform the task in a timely manner.

2.2. Vehicle-to-Pedestrian communications

In order to mitigate the problem of occluded pedestrian detection with LoS sensors, Vehicle-to-Pedestrians (V2P) wireless communication was leveraged to detect the presence of pedestrians. WiFi, Zigbee, and Ultra-Wideband (UWB) were used in [32–35] for V2P communication and alerting either drivers or pedestrians about anticipated collisions. [36] have proposed a framework for V2P communications via DSRC units with the goal of alerting both the pedestrians and the vehicle to a possible collision. The fusion of the car's perception and V2P communications was leveraged by [37]. Their solution relies on recognizing the occlusion by a moving vehicle and sending an alert to the pedestrian's device if detected via V2P communications.

Although V2P communications enhance the safety of occluded pedestrians by improving the detection rate, their main drawback

is that they are usually power-hungry and are apt to drain the battery of the pedestrian's device if used for extended periods of time. Yet another drawback is that V2P communications rely on inaccurate GPS readings to determine the distance between the pedestrian and approaching vehicles. Additionally, V2P communications do not scale well when multiple pedestrians are found in the street.

2.3. Collaborative perception

Collaborative perception in Vehicular Ad Hoc Networks (VANET) is used in pedestrian safety systems when a moving car fails to detect pedestrians using its on-board sensors and relies on remote sensors such as other cars' on-board cameras or street monitoring cameras to provide additional perception. Information is shared between vehicles in VANET using Vehicle-to-Vehicle (V2V) communication or through communication with Road Side Unit (RSU). [38] proposed a collaborative system that shares pedestrians' information when they are detected by another car's camera. The detecting car exchanges pedestrian location and speed with the blinded car(s). Their system has the advantage of enabling collaboration between cars to prevent pedestrian/car collisions.

Several projects attempt to enhance pedestrian detection at intersections by installing cameras and ranging sensors on light poles or RSUs. Once the pedestrians are detected, approaching vehicles are alerted to their presence. For example, [39–41] installed a camera in an RSU to detect pedestrians and to alert approaching vehicles. [42] and [43] suggested fusing input from installed cameras with thermal and LiDAR sensors to detect pedestrians at day and night. In lower cost mechanism, [44] installed piezoelectric elements at the beginning and end of crossing lines to detect pedestrians and to alert approaching vehicles through RSUs. The aforementioned approaches are expensive to deploy and, consequently, municipalities usually do not have the resources to install them at all locations. Besides, they only cover controlled intersections while many pedestrians are known to roads mid-block. Additionally, the alert messages are exchanged between RSU and approaching vehicles via DSRC which covers a large area causing network load and impairments of radio transmissions, various forms of interference, message propagation delays, and security concerns.

2.4. Putting parked cars to work

Parked cars have been used in VANET to relay safety message dissemination in areas with low traffic density. As an example, [45] proposed the idea of using parked cars as RSUs to improve VANET connectivity. Similarly, [17] showed that parked cars are useful to work as relay nodes in support of VANET communications. To increase road safety, [18] proposed that parked cars communicate with their moving counterparts as relay nodes to increase safety in low-density areas by multi-hopping the Cooperative Awareness Messages. Yet another technology that leverages the potential of parked cars is the recently proposed Vehicular Clouds [65].

Due to the vast panoply of their on-board sensors, parked cars can also be used as a sensing resource. [46] showed that parked cars can be used as sensing resources and that the CAN bus can be used to provide power to the sensors. Parked cars have been also used for detecting missing objects by [47] by instrumenting cars with RFID readers to detect tags attached to missing objects, then share the detection information with administrative centers. One of the drawbacks of RFID-based detection approaches is that they need a secure communication medium to protect users' privacy. Undoubtedly, using parked cars as a sensing resource is beneficial in terms of providing accurate and timely information.

2.5. Energy harvesting wearables

Energy harvesters such as piezoelectric elements were used in shoes to activate sensors from mechanical energy generated during walking [48]. Moreover, [49] developed a shoe module that can communicate with a smart-phone held by the user. Their work showed that the power produced by a single shoe is sufficient to transmit data from a Bluetooth module to the smart-phone. Such a module can be used to enable pedestrians to generate signals to be received by nearby receivers that operate on the same frequency as we proposed in this paper. Most importantly, they can transmit signals while harvesting power from their own motion rather than external batteries.

2.6. Short-range Received Signal Strength localization

Due to their simplicity and efficiency in terms of power consumption, Received Signal Strength (RSS) ranging approaches are commonly used in wireless localization [50]. However, because of its limited accuracy, RSS-based ranging is used mostly as a coarse-grain indicator, especially in long-range localization efforts. As pointed out by [51], the accuracy of RSS localization is surprisingly good at short ranges (within 1-3 meters) which makes it a good candidate to be used in ADOPT.

3. ADOPT: system assumptions

The main goal of this section is to spell out the basic system assumptions that underlie ADOPT. ADOPT relies on detecting radio frequency (RF) signals transmitted at each step while a pedestrian is walking. Many *wearable devices*, including smart-phones, wrist-bands, and shoes can detect human steps [52]. Since we aim to design a low-power and low-cost system, we focus on leveraging wearables that harvest energy from body motion. Specifically, we assume that the pedestrians (who might be children) are wearing shoes fitted with piezoelectric elements that provide a robust, lightweight, and inexpensive source of power for an in-shoe, battery-free, power generator [48,49]. As already mentioned, when a pedestrian's shoes touch the ground, a circuit is closed and a rudimentary transmitter embedded in the pedestrian's shoe is activated for a fraction of a second. The transmission range in this paper is assumed to be up to 3 meters.

We assume that the parked cars know their exact geographic location by interfacing with a digital map. In support of detecting the presence of pedestrians, cars are fitted with four low-power radio transceivers placed at the front and rear axles on each side of the car. These transceivers detect and measure the strength of RF signals transmitted by pedestrians' shoes. The detection range of each transceiver is assumed to be 3 meters in this paper. Recall that the four transceivers mentioned above, are integrated into, powered by, and synchronized to the intra-vehicle CAN bus [22].

The cars parked along the sidewalk are assumed to be aware of the distance between their right transceivers and the sidewalk. This distance can be estimated by using any on-board proximity sensor before stopping. The cars are assumed to be parked parallel to the sidewalk. This is assumed for convenience only. Indeed, if the cars are parked orthogonal to the sidewalk, they are assumed to be aware of the distance between their front or rear transceivers and the sidewalk. Notice that a car can detect its orientation with respect to the sidewalk using any rudimentary on-board navigation system or its inertial sensors.

The cars parked along the sidewalk self-organize into a linear vehicular network [53]. In this work, we refer to the resulting network as a *chain* of parked cars. Refer to Fig. 1 for an illustration. By consulting its on-board digital map, each car in the chain determines the width of the street and the speed limit. It also identifies

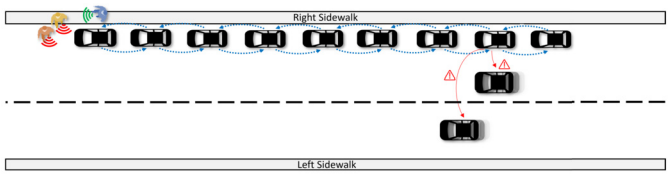

Fig. 1. Illustrating ADOPT: Parked cars detect occluded crossing pedestrians and alert approaching cars.

its position in the chain and the pseudonyms of its two adjacent neighbors. When a car is departing or joining the chain, a simple maintenance operation is performed to maintain the network [54].

It is important to note that since in an on-street parking situation, adjacent parked cars are, typically, a short distance away from each other [55], the tasks inherent to self-organization and maintenance of the chain of parked cars can be performed at low power using a suitable subset of transceivers such as Bluetooth Low Energy (BLE) or Zigbee.

We assume that when ADOPT is booted, there are no pedestrians in the street – pedestrians, if any, are all on the sidewalk. This assumption is non-essential and is made for convenience only. Similarly, we assume that pedestrians step into the street from the sidewalk *in front* of a parked car. If the pedestrians step into the street behind a given parked car, but in front of the next parked car in the chain, the latter will be responsible for undertaking the alerting actions. If there is no car parked behind, then the original parked car will undertake the alerting actions, as described in Section 6, using its rear transceivers instead of the front ones.

Alert messages indicating the presence of a crossing cohort are propagated backward along the chain of parked cars, as illustrated in Fig. 1. As they pass cars in the chain of parked cars, approaching cars will be alerted, using low-power communications, to the reported location (or locations) of crossing pedestrians.

Although not specifically designed with self-driving cars in mind, ADOPT can be easily implemented to run on self-driving cars. When such a car receives an ADOPT "Caution – pedestrian in the street" message, it complies by reducing its speed without delay using a control system such as the system proposed by [56]. However, at the moment, self-driving cars are not very common, and so ADOPT alerts human drivers by displaying appropriate messages on a dashboard digital map, attempting to minimize distraction. For this purpose, we assume an ADOPT app that is running in approaching cars. The app determines the speed reduction necessary to avoid collision with the crossing cohorts and displays the suggested speed on the dashboard.

4. Pedestrian classification and localization

The first task that parked cars need to undertake is to determine if there are pedestrians in the street. If no pedestrians are in the street all is well. Otherwise, the pedestrians have to be accurately localized and their crossing time estimated. Once this information is in hand, approaching cars are alerted to the presence of the crossing cohort. The main goal of this section is to provide the details of pedestrian classification and localization.

4.1. Pedestrian detection

Recall that, as mentioned in Section 3, with each step the pedestrians' shoes generate, for a fraction of a second, an RF signal with a known power T and a known frequency f [49]. When a pedestrian walks near a parked car, the transceivers in the car receive the signals generated by the pedestrian's shoes. We calculate the Received Signal Strength $RSS(Rx)$ at a generic transceiver Rx using the Free Space propagation model [57]:

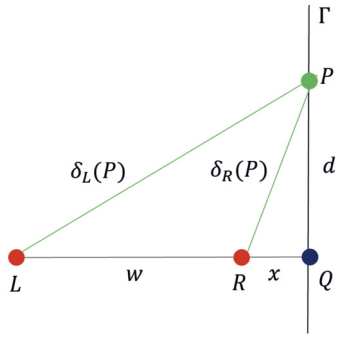

Fig. 2. Illustrating the proof of Lemma 1.

$$RSS(Rx) = \frac{T\gamma}{\delta_{Rx}^2}, \tag{1}$$

where T is the power of the transmitted signal, γ is an environmental constant, and δ_{Rx} is the distance between the pedestrian who transmits the signal and the transceiver Rx. The pedestrian is assumed to be detected if her δ_{Rx} is less than or equal the detection range of Rx.

4.2. Pedestrian classification

An important task that ADOPT undertakes is the *binary* classification of detected pedestrians: *on the sidewalk* or *in the street*. We begin by stating and proving a technical result, of an independent interest, that provides a simple criterion for classifying pedestrians.

Lemma 1. *Consider two points L and R in the plane and assume that the line segment LR they determine has length $w > 0$. Let Γ be an arbitrary line perpendicular to LR. Γ is the locus of all the points P for which*

$$\delta_L^2(P) - \delta_R^2(P) = constant, \tag{2}$$

where $\delta_L(P)$ and $\delta_R(P)$ are, respectively, the distance from P to the endpoints of the segment LR.

Proof. Let Q be the intersection of the (infinite) line through L and R with Γ and refer to Fig. 2. Assume, without loss of generality, that Q lies to the right of R. Denote by d the length of the segment PQ and by x the length of the segment RQ.

By applying the Pythagorean theorem to triangles LPQ and RPQ we write

$$\begin{cases} \delta_L^2(P) = (w+x)^2 + d^2 & \text{and} \\ \delta_R^2(P) = x^2 + d^2 \end{cases}$$

and consequently,

$$\delta_L^2(P) - \delta_R^2(P) = (w+x)^2 + d^2 - x^2 - d^2 = w^2 + 2wx. \tag{3}$$

Observe that the line Γ determines *uniquely* x and conversely. Specifically, for a given line Γ, x is a constant (that depends on Γ) and so the expression $w^2 + 2wx$ is a constant implying that $\delta_L^2(P) - \delta_R^2(P)$ is itself a constant.

Conversely, assume that

$$\delta_L^2(P) - \delta_R^2(P) = c$$

for some constant c. By (3), this implies that $w^2 + 2wx = c$ whereupon, solving for x yields

$$x = \frac{c - w^2}{2w}.$$

In turn, this uniquely determines the line Γ, and the proof of Lemma 1 is complete.

Lemma 1 justifies a simplification of notation. Specifically, when the line Γ is clear from the context, the expression $\delta_L^2(P) - \delta_R^2(P)$ will be written, simply, as $\delta_L^2 - \delta_R^2$ as its value is independent of the choice of the point P on Γ.

We now state and prove an important consequence of Lemma 1 that will be used as a building block of our binary classification of pedestrians: *on the sidewalk* or *in the street*. In order to state our result, we find it convenient to inherit the notation of Lemma 1.

Theorem 2. *Consider an arbitrary line Γ and assume a transmitter placed at an arbitrary point P on Γ. Let RSS(L) and RSS(R) be, respectively, the Received Signal Strength received by two transceivers placed at L and R. Then, regardless of the location of P on Γ, we have*

$$\frac{1}{RSS(L)} - \frac{1}{RSS(R)} = c(\Gamma) \tag{4}$$

where $c(\Gamma)$ is a constant that depends on Γ.

Proof. By (1) the Received Signal Strengths $RSS(L)$ and $RSS(R)$ received by two transceivers placed at L and R are, respectively,

$$RSS(L) = \frac{T\gamma}{\delta_L^2} \quad \text{and} \quad RSS(R) = \frac{T\gamma}{\delta_R^2}, \tag{5}$$

where T is the power of the transmitted signal and γ is an environmental constant.

Now, equations (2) and (5), combined allow us to write

$$\begin{aligned} \frac{1}{RSS(L)} - \frac{1}{RSS(R)} &= \frac{\delta_L^2}{T\gamma} - \frac{\delta_R^2}{T\gamma} \\ &= \frac{\delta_L^2 - \delta_R^2}{T\gamma} \\ &= \frac{w^2 + 2wx}{T\gamma} \quad [\text{by (3)}] \\ &= c(\Gamma), \end{aligned} \tag{6}$$

where the last step of the derivation follows because there is a one-to-one correspondence between Γ and x.

Discussion. Assume a car parked parallel with the edge of the sidewalk. Theorem 2 establishes a one-to-one correspondence between a subset of real numbers and the set of lines in the plane parallel to the edge of the sidewalk. This is to say, to each line Γ in the plane parallel to the edge of the sidewalk, there corresponds a unique real number $c(\Gamma)$ and, conversely, to each real number there corresponds exactly one line in the plane parallel to the edge of the sidewalk. One of these lines is of a special interest: this is the edge of the sidewalk. As the next result shows, the resulting constant, c_0 acts as a discriminant between locations on the sidewalk and in the street.

Corollary 3. *Let the line Γ_0 coincide with the edge of sidewalk, assumed rectilinear. There is a unique constant c_0 such that the pedestrian (assumed to carry a transmitter) is on the sidewalk or in the street depending on whether $\frac{w^2+2wx}{T\gamma} > c_0$ or $\frac{w^2+2wx}{T\gamma} < c_0$.*

Proof. Let x_0 be the distance between R and the edge of the sidewalk and write

$$c_0 = \frac{w^2 + 2wx_0}{T\gamma} \tag{7}$$

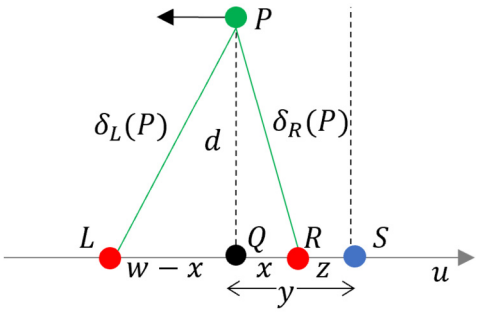

Fig. 3. Illustrating the notation for the proof of Lemma 4.

Let Γ be a vertical line passing through an arbitrary point on the sidewalk and let x be the distance between R and the intersection point of the line LR with Γ. Clearly, $x > x_0$ and, consequently,

$$\frac{w^2 + 2wx}{T\gamma} > c_0.$$

Thus, for points on the sidewalk the expression $\frac{w^2+2wx}{T\gamma}$ is larger than c_0. The proof is similar for points in the street.

The one-to-one correspondence discussed above is a very useful property because in order to determine if a pedestrian is on the sidewalk, all we have to do is to evaluate the left-hand side of (4) and to compare the result to the value of c_0 from (7). This, in fact, is tantamount to a coarse-grain binary localization of pedestrians: on the sidewalk, or else in the street.

4.3. Pedestrian localization

Pedestrians that are classified as *in the street* have to be localized more accurately, as we are about to explain. Referring to Fig. 3, consider a pedestrian P and let point Q be the projection of P onto the line determined by L and R. We assume, without loss of generality, that Q lies between L and R. We assume that the pedestrian crosses the street by walking in a straight line parallel to the front of the parked car (i.e., perpendicular to the sidewalk). Let d be the length of the line segment PQ (that is, the vertical distance between the location of the pedestrian and the line LR. Further, let w be the width of the parked car, let x be the length of the line segment QR, let z be the distance from R to the sidewalk, and write $y = x + z$.

Now, elementary geometry confirms that y has the following expression

Lemma 4.

$$y = \frac{w}{2} + z - \frac{T\gamma}{2w}\left[\frac{1}{RSS(L)} - \frac{1}{RSS(R)}\right]. \tag{8}$$

Proof. By using the Pythagorean theorem in the triangles PQL and PRQ we can write:

$$\begin{cases} \delta_L^2 = (w-x)^2 + d^2 & \text{and} \\ \delta_R^2 = x^2 + d^2 \end{cases}$$

and so:

$$\delta_L^2 - \delta_R^2 = (w-x)^2 - x^2 = w^2 - 2wx. \tag{9}$$

From (1),

$$\begin{cases} \delta_L^2 = \frac{T\gamma}{RSS(L)} & \text{and} \\ \delta_R^2 = \frac{T\gamma}{RSS(R)} \end{cases}$$

by plugging these values into (9), we obtain

$$\frac{T\gamma}{RSS(L)} - \frac{T\gamma}{RSS(R)} = w^2 - 2wx.$$

Solving for x yields

$$\begin{aligned} x &= \frac{w^2}{2w} - \frac{T\gamma}{2w}\left[\frac{1}{RSS(L)} - \frac{1}{RSS(R)}\right] \\ &= \frac{w}{2} - \frac{T\gamma}{2w}\left[\frac{1}{RSS(L)} - \frac{1}{RSS(R)}\right] \end{aligned} \tag{10}$$

Finally,

$$\begin{aligned} y &= x + z \\ &= \frac{w}{2} + z - \frac{T\gamma}{2w}\left[\frac{1}{RSS(L)} - \frac{1}{RSS(R)}\right], \end{aligned} \tag{11}$$

as claimed.

Now, referring again to Fig. 3, it is clear that since the pedestrians are crossing the street in a direction perpendicular to the sidewalk, in order to specify the location of a crossing pedestrian, it suffices to specify the value of y, as above, along with the value of d, the vertical distance to the front of the parked car.

In order to determine d, we compute the area of the triangle PLR in two different ways:

- First, evidently, $Area(PLR) = \frac{w \cdot d}{2}$;
- Second, writing $p = \frac{\delta_L + \delta_R + w}{2}$, the same area can be expressed as

$$Area(PLR) = \sqrt{p(p-\delta_R)(p-\delta_L)(p-w)}$$

Consequently,

$$\frac{w \cdot d}{2} = \sqrt{p(p-\delta_R)(p-\delta_L)(p-w)},$$

which, upon solving for d, yields:

$$d = \frac{2}{w}\sqrt{p(p-\delta_R)(p-\delta_L)(p-w)}. \tag{12}$$

5. Estimating the time to cross

Recall that a crossing cohort is a group of pedestrians crossing together at the same location. Instead of dealing with each member of the cohort individually, we only concern ourselves with the *tail* of the cohort, defined as the last pedestrian in the cohort. It is clear that if the tail of the cohort has crossed safely, then all pedestrians in the cohort have crossed safely, too. It is important to note that ADOPT is *privacy-aware* as we are only interested in the location of the tail of the cohort, and not in the actual person that happens to be the last in the cohort.

We now define the tail of a crossing cohort more formally. Recall that the parameter y, defined in Lemma 4 keeps track of the current distance of a crossing pedestrian to the sidewalk she just departed. Formally, then, at each moment in time, the tail of the crossing cohort is the pedestrian with

$$\min\{y|\ \text{pedestrian classified as in the street}\}. \tag{13}$$

Notice that the tail may change dynamically, either because new pedestrians joined the cohort, a pedestrian turns back after starting crossing or, simply, because some folks in the cohort walk faster than others. ADOPT updates the tail of the crossing cohort every second.

To manage the tail of a cohort, ADOPT needs to process signals from several pedestrians simultaneously. To accomplish this, the transceivers in the parked car sample frequency f on which the pedestrians' shoes are transmitting signals, m times per second. Conceptually, this means that each second is partitioned into m slots. Assume that each pedestrian takes one step per second, and that each step generates one transmission. For all practical purposes, this transmission occurs, randomly, in one of the m slots discussed above. Now, suppose that there are k, $(k \geq 1)$, pedestrians in the crossing cohort. We have just set up a "balls-into-bins" model involving k balls and m bins. If two or more pedestrians are transmitting in the same time slot, a collision occurs and the outcome cannot be disambiguated.

We are interested to assess the expected number of "clear" transmissions, where one single transmission occurs in a given time slot. For arbitrary i, $(1 \leq i \leq k)$, let X_i be the indicator random variable that takes on the value 1 if, in a given second, slot i sees a clear transmission and 0 otherwise. It is easy to see that

$$\Pr[X_i = 1] = \left(1 - \frac{1}{m}\right)^{k-1}$$

and that the expected number, $E[M]$, of clear transmissions is

$$\begin{aligned} E[M] &= E[X_1 + X_2 + \cdots + X_k] \\ &= E[X_1] + E[X_2] + \cdots + E[X_k] \\ &= \Pr[X_1] + \Pr[X_2] + \cdots + \Pr[X_k] \\ &= k\left(1 - \frac{1}{m}\right)^{k-1}. \end{aligned}$$

As an illustration, if a given cohort were to contain $k = 8$ pedestrians, and assuming that frequency f is sampled 50 times per second, we would expect to see $E[M] = 8 \times \left(1 - \frac{1}{50}\right)^7 = 8 \times (\frac{49}{50})^7 \approx 6.9$ clear transmissions each second.

With this in mind, consider the time ruled into seconds and assume that in second t, the tail of the current crossing cohort was located at $y(t)$ and its current speed, $v(t)$, has been estimated. The *remaining time to cross* at time t, $\Delta(t)$, can be estimated as

$$\Delta(t) = \frac{W - y(t)}{v(t)}, \tag{14}$$

where W is the width of the street that the pedestrians are crossing.

We need to show how these parameters are updated in the next second, $t+1$. We begin by identifying all clear transmissions in second $t+1$ and, using equation (13), we obtain the location, $y(t+1)$, of the current tail. We distinguish between the following cases:

Case 1: $y(t) < y(t+1)$**.**

Evidently, in this case, the new tail is closer to the opposite sidewalk. It follows that no new pedestrian has joined the cohort in this second. In this case, it is natural to update the cohort parameters as follows:

- $v(t+1) = y(t+1) - y(t)$ m/s;
- $\Delta(t+1) = \frac{W - y(t+1)}{v(t+1)}$.

Case 2: $y(t) > y(t+1)$**.**

In this case, it is clear that one or more pedestrians have joined the cohort and, consequently, the new tail must be selected from among the pedestrians who have just joined the cohort. There is a complication: we cannot update the speed of the tail, because the tail is new. Instead, we assign to the new tail, tentatively, the average crossing speed. The cohort parameters are updated as follows:

- $v(t+1) = v_0$, where v_0 is an estimate of the average pedestrian speed;
- $\Delta(t+1) = \frac{W - y(t+1)}{v(t+1)}$.

6. Safety zone and message propagation

ADOPT involves two types of car-to-car messages, each with its own semantics:

- *Alert messages:* are sent by the parked car that detects a crossing cohort with the intention of establishing a *Safety Zone*, as we are about to describe;
- *Caution messages:* are messages sent by the parked cars in the Safety Zone to alert approaching cars to the presence of crossing pedestrians.

These to types of messages will be discussed in Subsections 6.1 and 6.2, respectively.

6.1. Alert messages

Referring to Fig. 4, assume, without loss of generality, that car A detects a crossing cohort at time t. Proceeding as discussed in Section 5, car A estimates the remaining time, $\Delta(t)$ (see (14)), it takes the tail of the cohort to cross the street. Using this information, car A determines the distance, $D(t)$, the alert messages will have to be propagated along the chain as follows:

$$D(t) = [\Delta(t) + r] \cdot v_{max}, \tag{15}$$

where r is the *driver reaction* time, estimated to be between 1.24 seconds and 2 seconds [58]. If self-driving cars are considered, then r is set to zero, since the driver reaction time is a human factor and does not affect self-driving cars. Finally, car A propagates the alert message containing: its own location, $x(A)$, on the digital map, the current time, t, and the Distance-to-Live $D(t)$ of the alert message in meters.

Referring to Fig. 4 again, the area of length $D(t)$, defined in (15), starting at car A and running down the chain of parked cars is called the *Safety Zone* associated with the crossing cohort detected by car A. Each parked car in the chain of parked cars, upon receiving the alert message originated by car A, compares its own location with that of A and determines if the distance from A is smaller than or equal to $D(t)$. If so, it marks itself as being in the Safety Zone and propagates the alert message further along the chain. In the case that the distance between two consecutive cars is large, the low-power communication cannot be used to deliver the alert message. Instead, DSRC is assumed to deliver it to the next parked car.

As an illustration, in Fig. 4, assume that car C has just received the alert message from the previous car in the chain. Let $x(A)$ and $x(C)$ be the x-coordinates of A and C, respectively. If $|x(A) - x(C)| \leq D(t)$ then C remembers that it belongs to the Safety Zone and propagates the message further down the chain. Continuing in this way, the alert message will reach, eventually, car B. When car B receives the alert message, it finds that $|x(A) - x(B)| > D(t)$, and so it discards the message. As illustrated in Fig. 4, car B is not in the Safety Zone.

6.2. Caution messages

Each parked car inside the Safety Zone is tasked with broadcasting a "Caution – pedestrians in the street" (Caution, for short) message to approaching cars. This broadcast must be done at low power, as illustrated in Fig. 4, using BLE or Zigbee, as passing cars are a short distance away from parked cars. The Caution message contains:

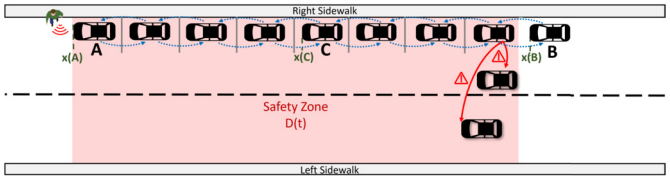

Fig. 4. Parked cars in the Safety Zone propagate alert messages within the estimated propagation distance to alert approaching cars.

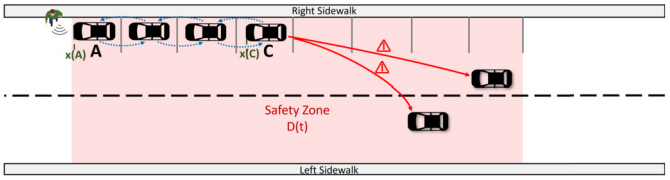

Fig. 5. The Last car in the chain delivers the Caution message to the approaching car via DSRC if the chain length is less than $D(t)$.

- the location $x(A) + d$ of the crossing cohort, where d was computed in (12);
- the time, $t + \Delta(t)$, at which the cohort is expected to have crossed the street.
- the direction of the alert message indicated by one bit. By convention, if the alert message is intended for cars moving northbound, the direction bit will be set.

In the unlikely event where many cars in the chain of parked cars depart, leaving big gaps in the chain, as shown in Fig. 5, the last car in the chain uses its DSRC transmitter to broadcast the Caution message to inform approaching cars of the location of the crossing cohort. As an illustrated in Fig. 5, car C with $|x(A) - x(C)| < D(t)$ does not detect any car behind it. Hence, car C will use its DSRC transmitter to broadcast the "Caution" message at a distance of $D(t) - x(C)$, where $x(C)$ is the location of C.

In the next second, $t+1$, a new estimate $D(t+1)$ is made as discussed in Section 5. If $D(t+1) > D(t)$ then an updated alert message is sent with Distance-to-Live $D(t+1)$. Otherwise, no action is needed.

7. How approaching cars determine a safe speed

The main goal of this section is to show how approaching cars, alerted to the presence of crossing cohorts, adjust their speed in such a way that they avoid colliding with the crossing pedestrians.

Our approach is novel and is based of a new way of looking at the time-space diagram (see the Appendix for a refresher).

Referring to Fig. 6, consider a car moving North-bound along a street. At time $s1$, the car is inside the Safety Zone, and receives a "Caution – pedestrians in the street" message alerting it to a crossing cohort at location $(0, L1)$. Upon receiving an alert message, the car will compare the direction bit with its actual direction of movement. If the car is moving South-bound, it will ignore the alert message. Assume that the location of the car at time $s1$ is $(s1, C)$ and that the cohort will finish crossing the street at time $e1$.

Proceeding as indicated in Subsection A.2 of the Appendix, the approaching car computes the maximum safe speed:

$$v_{safe} = \min\left\{v_{max}, \frac{L1 - C}{e1 - s1}\right\}, \tag{16}$$

where v_{max} is the speed limit along the street.

Traveling at this safe speed North-bound, the approaching car receives, at time $s2$, a second "Caution – pedestrians in the street" message alerting it to the presence of a second crossing cohort.

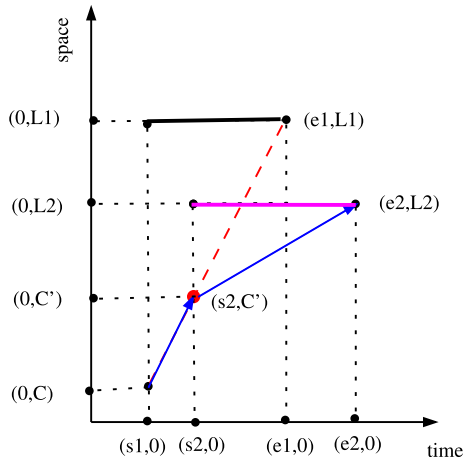

Fig. 6. Illustrating the computation of the safe average speed in the case of two crossing cohorts.

This cohort crosses the street at location $(0, L2)$ and will finish crossing at time $e2$. How should the car change its speed to avoid an accident?

In order to answer this question, the first task is to determine the location, $(s2, C')$ of the car at time $s2$. This can be done by noting that v_{safe} in equation (16) can we written as

$$\frac{L1 - C}{e1 - s1} = \frac{C' - C}{s2 - s1}.$$

Solving for C' yields:

$$C' = C + \frac{(L1 - C)(s2 - s1)}{e1 - s1}.$$

With C' firmly in hand, the car updates the current safe speed v_{safe} in (16) as follows:

$$\begin{aligned} v_{safe} &= \min\left\{v_{safe}, \frac{L2 - C'}{e2 - s2}\right\} \\ &= \min\left\{v_{max}, \frac{L1 - C}{e1 - s1}, \frac{L2 - C'}{e2 - s2}\right\}. \end{aligned} \tag{17}$$

The justification of (17) is simple. The car needs to select the largest average safe speed and this is the smallest of the slopes of the lines segments determined by the points $(s2, C')$ and $(e1, L1)$ on the one hand, and the points $(s2, C')$ and $(e2, L2)$ on the other.

At time $e1$, the car realizes that the first cohort has finished crossing the street and will adjust its speed again:

$$v_{safe} = \min\left\{v_{max}, \frac{L2 - C'}{e2 - s2}\right\}. \tag{18}$$

In Fig. 6,

$$\min\left\{v_{max}, \frac{L1 - C}{e1 - s1}, \frac{L2 - C'}{e2 - s2}\right\} = \min\left\{v_{max}, \frac{L2 - C'}{e2 - s2}\right\}$$

and, consequently, the car continues driving at the same speed.

Next, at time $e2$, the car realizes that the second cohort has finished crossing and so it will adjust its speed again:

$$v_{safe} = \min\{v_{max}\} = v_{max}, \tag{19}$$

essentially, reverting to the maximum allowed speed.

The same procedure is then continued, exactly as described, should other "Caution – pedestrians in the street" be received by the car in the future.

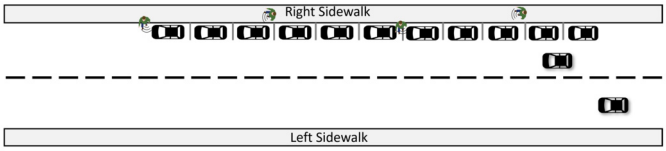

Fig. 7. An instance of the ADOPT simulation model.

Table 1
A summary of simulation parameters.

Parameter	Value
RF signal frequency f	2.4 GHz
Transmission Power T	2 mW
Detection Range	up to 3 meters
Street width W	12.8 m
Distance from R transceiver to the sidewalk z	0.4 m
Number of detected pedestrians/sec $[\mu, \sigma]$	[1.8,1.4]
Pedestrians speeds $[\mu, \sigma]$	[1.15, 0.13] m/sec
Average speed v_0	1.2 m/sec
Number of crossing pedestrians/sec $[\mu, \sigma]$	[0.11, 0.32]
Street speed limit v_{max}	15 m/sec
Simulation step length	1 sec
Simulation steps	3600 sec (1 hour)

8. Simulation and results

In this section, we describe how ADOPT simulation model is developed and how we evaluated ADOPT performance.

8.1. Simulation model

We validated the theoretical findings of ADOPT by testing them on simulated traffic data. For this purpose, we used Simulation of Urban MObility (SUMO) [59] to generate pedestrian and car traffic data for the ADOPT simulation model illustrated in Fig. 7.

Our simulation model consists of a *one-way* street with a roadside parking lane on the right side of the street and sidewalks on both sides. Approaching cars enter at the end of the street and exit from the opposite end.

SUMO is also known as a microscopic simulation for pedestrian mobility. In our simulation model, the pedestrians are not restricted to crossing at intersections but, indeed, they may cross *midblock* a prevalent behavior [14]. In SUMO, pedestrian are set by default to slowdown their speed before crossing to make sure the street is clear and stop if there passing cars. We enforced pedestrians to ignore the approaching cars. Hence, they do not stop or hesitate before crossing the street. By this setting, we collect more data when the car approaches while a pedestrian start crossing the street. Moreover, SUMO has implemented a collision avoidance model to force vehicles to reduce their speed if there are crossing pedestrians. We disabled this mode before we generated the vehicular traffic to measure the effect of receiving the caution message correctly.

For the reader's convenience, we summarize the simulation parameters in Table 1.

We modeled pedestrians' radio signals using equation (1) by setting a constant transmission power equals to 2 mW transmitted from their actual locations. We then obtained the actual Euclidean distances δ_{Rx} between the pedestrian locations and the four transceivers located at the four corners of cars. We assumed that the pedestrian is detected by a transceiver if the distance between the transceiver and the pedestrian is less than or equal 3 meters.

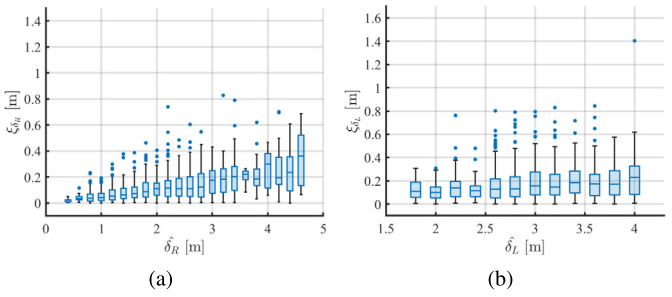

Fig. 8. Absolute error of estimated distances δ_R and δ_L against the actual distances (a) $\hat{\delta_R}$ and (b) $\hat{\delta_L}$.

For the communication between parked cars and approaching cars, we assume the cars are communicating using low-power communication modules such as BLE which has been proven to provide a reliable V2V communication [60]. Based on that, when the car enters the Safety Zone, we assume that it receives the "caution message" from the closest parked car.

The data we collected from SUMO are as follows: street and sidewalk dimensions, pedestrians' locations, pedestrians' speeds, parked cars' locations and dimensions, and approaching cars' speed and location at each time step. Data collected from SUMO is our ground truth, i.e., "actual", information about pedestrians and cars traffic.

8.2. Modeling RSS noise

In real-life situations, RSS measurements experience random fluctuations due to hardware-based parameters such as thermal noise, or due to the natural behavior of the signal as it is reflected by the ground [61]. Being close to the ground, we assume that there are no obstacles between the pedestrians' shoes and the transceivers.

We modeled the uncertainty in the RSS produced by receiving either more or less power than the original RSS as a Gaussian random variable Φ_σ with zero mean and a standard deviation σ as follows:

$$RSS'(Rx) = RSS(Rx) + \Phi_\sigma$$

where RSS' is the noisy received signal strength at a generic transceiver Rx. We set σ to 0.3 mW since we only consider short transmission ranges and near-the-ground communication. The added noise affects the distance we estimate based on the RSS. We measured the impact of noise by calculating the absolute error ξ of the estimated distance at each transceiver $RSS(R)$ and $RSS(L)$ where $\xi_{\delta_R} = |\hat{\delta_R} - \delta_R|$ and $\xi_{\delta_L} = |\hat{\delta_L} - \delta_L|$. Fig. 8 shows the distribution of the absolute errors in distance estimated from $RSS'(R)$ and $RSS'(L)$ plotted against the actual distances (a) $\hat{\delta_R}$ and (a) $\hat{\delta_L}$ obtained from SUMO respectively. Note that the errors shown are observed at every 0.2-meters window. Results showed that the added noise causes minor distance estimation errors in ranges near the transceivers, but the errors increase as the pedestrians move away from the transceivers.

As the noise affects the RSS at both transceivers, it also affects the result of (6). Consequently, the noise impacts the one-to-one mapping, discussed in Section 4, between the set of lines parallel to the edge of the sidewalk and the $c(\Gamma)$ values as each line will have many $c(\Gamma)$ values. To determine the range of inaccuracy in $c(\Gamma)$, we defined a 0.2-meters window of the horizontal position before and after the sidewalk and aggregated the calculated noisy $c(\Gamma)$ from $RSS'(L)$ and $RSS'(R)$ at each window as we show in Fig. 9(a). To compare the noisy $c(\Gamma)$ with the noise-free $c(\Gamma)$, we show in the same figure the noise-free $c(\Gamma)$. The results showed

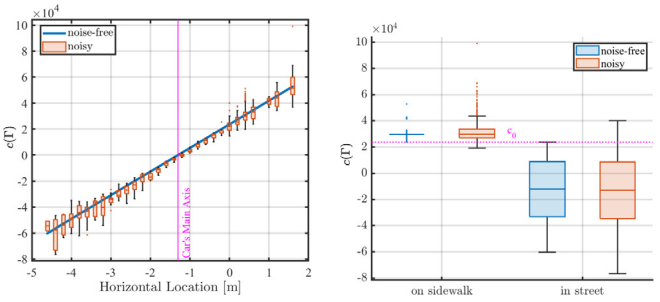

(a) *The noise produces multiple $c(\Gamma)$ values for the same parallel line to the sidewalk while the actual $c(\Gamma)$ is unique for each line.*

(b) *Distribution of $c(\Gamma)$ of pedestrians' signals per pedestrian's class (on the sidewalk and in the street). c_0 is used as a threshold to classify pedestrians.*

Fig. 9. Effect of noise on $c(\Gamma)$.

that the noise impacts the $c(\Gamma)$ if pedestrians are far from the main axis of the car (i.e. middle of the LR line segment), while it has a lower impact near the LR midpoint the pedestrians are close to both transceivers and $c(\Gamma)$ is almost zero. This affected also the classification based on the threshold c_0. Referring to Fig. 9(b), all $c(\Gamma)$ values of pedestrians walking on sidewalk are greater than c_0. Similarly, all $c(\Gamma)$ values of pedestrians who are in the street are less than c_0. The variation of $c(\Gamma)$ values shows that even though pedestrian location varies inside the sidewalk, they are identified to be inside the sidewalk as long as their $c(\Gamma)$ is greater than c_0. This Also proofs that even though the pedestrian may not walk in straight lines, she will be classified correctly. On the other hand, with the noisy $c(\Gamma)$, several $c(\Gamma)$ values of pedestrians walking on the sidewalk are less than c_0, and several $c(\Gamma)$ values of pedestrians walking in the street are greater than c_0.

8.3. Evaluation results

We evaluated the performance of ADOPT in two scenarios:

- **Scenario 1 – Noise-free mode:** in which we performed pedestrian classification and crossing time estimation using the actual data generated by SUMO;
- **Scenario 2 – Noisy mode:** in which we performed pedestrian classification and crossing time estimation using noisy RSS to have a more realistic evaluation.

We demonstrate the performance of ADOPT in both scenarios above. The overall performance of pedestrian classification is presented in Table 2. The accuracy of pedestrian classification in the noise-free mode was 100% accuracy, while the accuracy dropped to 93.25% in the noisy mode.

The other metrics we use to empirically evaluate the performance of ADOPT are: the accuracy of pedestrian localization, the accuracy of crossing time estimation, the accuracy of the remaining crossing time, as well as the accuracy of the Safety Zone size. We use Root Mean Squared Error (RMSE) to measure the accuracy of these estimations. We show the overall result of the RMSE in Table 3. We notice here that the RMSE of ADOPT estimations in the noise-free mode is low. However, in noisy mode the RMSE increases for the all estimations. The details of the evaluation will be explained later in this section.

In the following, we present the details of ADOPT evaluation and the results. Specifically, in Subsection 8.3.1 we discuss the accuracy of pedestrian classification; in Subsection 8.3.2 we discuss the accuracy of pedestrian localization, once they are in the street; the accuracy of pedestrian street traversal speed is discussed in Subsection 8.3.3; the accuracy of the remaining crossing

Table 2
Overall Accuracy of Pedestrian Classification.

		Predicted Class (noise-free mode)		Predicted Class (noisy mode)	
		in street (positive)	on sidewalk (negative)	in street (positive)	on sidewalk (negative)
Actual Class	in street (positive)	340 (TP)	0 (FN)	316 (TP)	24 (FN)
	on sidewalk (negative)	0 (FP)	1216 (TN)	81 (FP)	1135 (TN)
Accuracy		100%		93.25%	

Table 3
ADOPT Estimation RMSE.

RMSE	noise-free mode	noisy mode
E_y	0.00 m	0.26 m
E_d	0.00 m	0.24 m
E_v	0.05 m/sec	0.11 m/sec
E_Δ	0.51 sec	1.21 sec
E_D	12.79 m	42.23 m

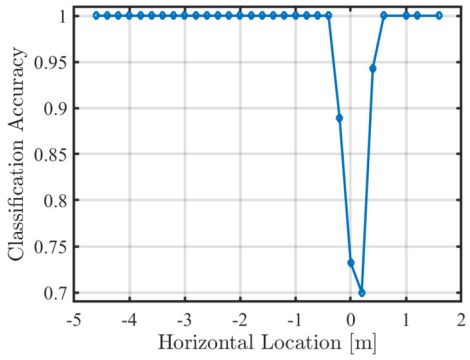

Fig. 10. Aggregated classification accuracy at horizontal locations before and after the edge of the sidewalk.

time is discussed in Subsection 8.3.4; the accuracy of establishing the Safety Zone is discussed in Subsection 8.3.5. Finally, Subsection 8.3.6 offers an end-to-end evaluation of ADOPT.

8.3.1. Accuracy of pedestrian classification

We evaluated the accuracy of pedestrian classification as *on the sidewalk* or *in the street* by using the following formula:

$$accuracy = \frac{TP + TN}{TP + TN + FP + FN} \times 100 \tag{20}$$

where

- TP (True Positive): is the total number of pedestrians that were correctly identified to be in the street;
- TN (True Negative): is the total number of pedestrians that were correctly identified to be on the sidewalk;
- FP (False Positive): is the total number of pedestrians incorrectly classified as in the street; and,
- FN (False Negative): is the total number of pedestrians incorrectly identified as on the sidewalk.

We obtained the ground truth of pedestrians classes directly from SUMO generated data.

To investigate the impact of noise on the classification performance in noisy mode, in Fig. 10 we plot the classification accuracy against the horizontal location (i.e. the position of lines that are parallel to the edge of the sidewalk) of the transmitted signal from the edge of the sidewalk that is indicated with value 0. Locations with negative values are in the street while locations with positive values are on the sidewalk. We noticed that the classification accuracy only drops when the transmitted signal is within few decimeters away from the edge of the sidewalk (i.e. location 0).

To better understand why the accuracy drops around the horizontal location 0, we investigated the accuracy metrics TP, FP, TN, FN, defined above in more detail. Referring to Fig. 11(a), the accuracy drops when we have FP and FN due to the noisy $c(\Gamma)$ (denoted by $c(\Gamma)'$). We noticed that FP classification occurs if $c(\Gamma)$ is less than c_0 and, at the same time, $c(\Gamma)'$ is greater than c_0. This means we have FPs if the noise generates $c(\Gamma)$ above the threshold c_0 while the actual $c(\Gamma)$ is lower than the threshold. Similarly, FN classifications occur if $c(\Gamma)$ is greater than c_0 and, at the same time, $c(\Gamma)'$ is less than c_0. This means we have FN if the noise generated $c(\Gamma)'$ below the threshold c_0 while the actual $c(\Gamma)$ is above the threshold. From the figure, we can see that this happens only in a limited area around c_0. To translate this to spatial data, in Fig. 11(b) we plotted $c(\Gamma)'$ corresponding to the horizontal location of the transmitted signal.

Obviously, high FN puts pedestrians at the risk as they enter the street and ADOPT does not alert the approaching cars. On the other hand, high FP results in flooding the approaching vehicles with incorrect alert messages while the pedestrians are on the sidewalk. To assess where ADOPT has miss-classification, we define our metric False Positive Per Location FPPL and False Negative Per Location FNPL where FPPL is the percentage of FP per horizontal location aggregated at each 0.2 meters, and FNPL is the percentage of FN per horizontal location aggregated at each 0.2 meters as well. Fig. 11(c) shows that FNPL is high only at locations situated a few decimeters away from the edge of the sidewalk. Moreover, ADOPT has higher FPPL a few decimeters away from the edge of the sidewalk. In conclusion, the ADOPT pedestrian classification scheme is able to classify pedestrians accurately even in the presence of noisy signals.

8.3.2. Accuracy of pedestrian localization

To measure the overall accuracy of pedestrian localization, we evaluated E_d and E_y, where E_d is the RMSE of location of pedestrians in front of the parked car (the vertical distance of the pedestrian) and E_y is the RMSE in estimating the pedestrian's distance from the edge of the sidewalk (the horizontal distance of crossing pedestrians). We evaluated E_d as follows:

$$E_d = \sqrt{\frac{\Sigma_{j=1}^{M}(\hat{d}_j - d_j)^2}{M}}$$

where M is the total number of received signals and $\hat{d}_j$ and d_j are, respectively, the actual and estimated vertical distances of the received signal. Similarly, we evaluated E_y as follows:

$$E_y = \sqrt{\frac{\Sigma_{j=1}^{M_s}(\hat{y}_j - y_j)^2}{M_s}}$$

where M_s is the total number of received signals that are actually detected in the street. $\hat{y}_j$ and y_j are the actual and estimated

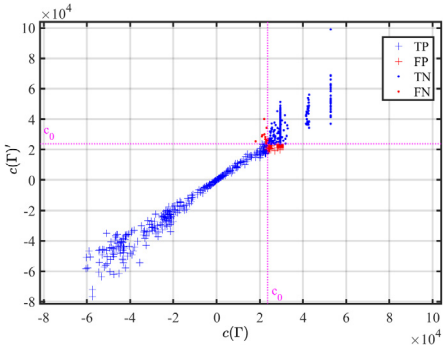

(a) *Detailed classification accuracy based on* $c(\Gamma)$ *and* $c(\Gamma)'$

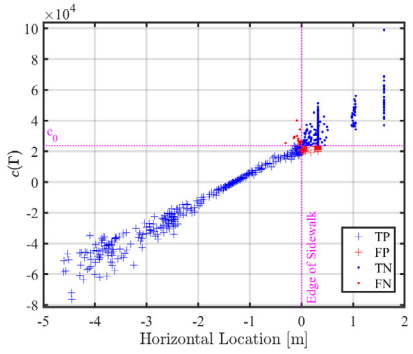

(b) *Detailed classification accuracy at horizontal locations before and after the edge of the sidewalk*

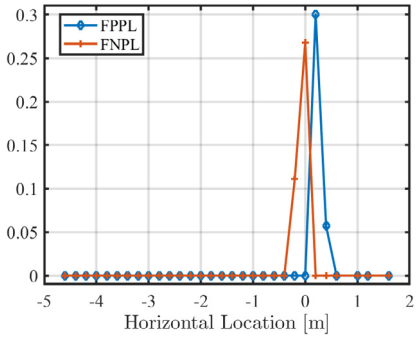

(c) *FPPL and FNPL are high only within 1 meter before and after the edge of the sidewalk with noisy signals.*

Fig. 11. ADOPT performance in pedestrian classification.

horizontal distances. Recall that y is only calculated when a pedestrian is classified as in the street. ADOPT estimation errors E_d and E_y were 0 meter in the noise-free mode, and less than 0.3 meters in the noisy mode as we show in Table 3.

To show the result in detail, we determined a 0.2-meters window of $\hat{d}$. Fig. 12(a) shows that the aggregated absolute error $\xi_d = |\hat{d} - d|$ is zero in the noise-free mode and does not exceeds 1.5 meters in the noisy mode.

Similarly, we determined a 0.2-meters window of $\hat{y}$ to observe the absolute error at each window. The absolute error of y is $\xi_y = |\hat{y} - y|$. Fig. 12(b) shows that the estimation of y in the noise-free mode is accurate since we have zero aggregated error. However, the aggregated error increases in noisy mode. The errors are lower as pedestrians start crossing the street because they are closer to

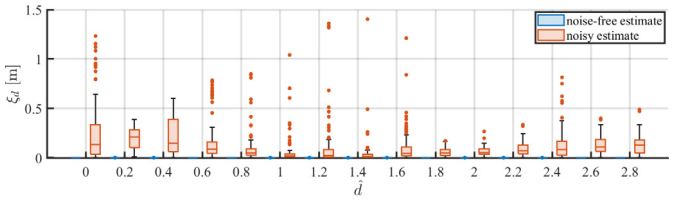

(a) ξ_d *against* $\hat{d}$

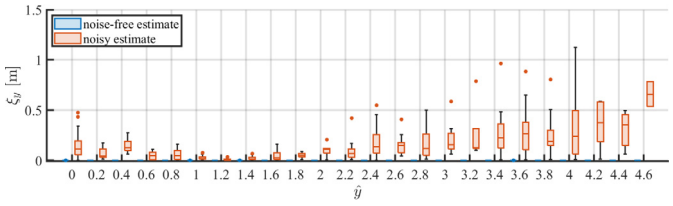

(b) ξ_y *against* $\hat{y}$

Fig. 12. Distribution of localization error against the actual location.

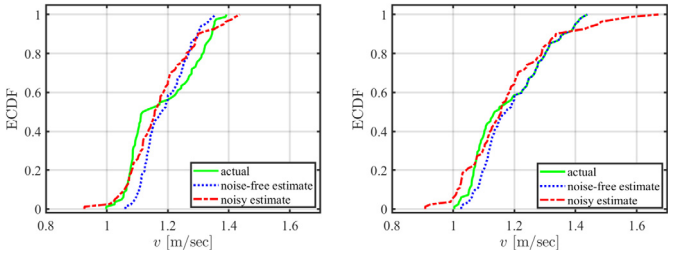

(a) *Dynamic Cohort Size* (b) *Fixed Cohort Size*

Fig. 13. ECDF of Pedestrian Speeds.

the main axis of the car (i.e. around $y = 1.3$) and the noise is low in this area as we showed previously in Fig. 9(a).

8.3.3. Accuracy of crossing speed estimation

We used RMSE to measure the overall accuracy of estimating the pedestrian's speed v as follows:

$$E_v = \sqrt{\frac{\Sigma_{i=1}^{N}(\hat{v}_i - v_i)^2}{N}}$$

where N is the total number of pedestrians generated in the simulation, and $\hat{v}_i$ and v_i are, respectively, the actual and the estimated speed of each pedestrian who was actually in the street. We chose to average the speed of each pedestrian individually because one pedestrian may vary her speed in SUMO. The results show that ADOPT RMSE in crossing speed estimation E_v was less than 1 meter/sec in noise-free mode while it has higher error in the noisy mode. Fig. 13(a) shows the Empirical Distribution Cumulative Function ECDF of the actual speeds, that are retrieved from SUMO, and the speeds that we estimate in noise-free and lastly the speed estimate in the noisy mode. The results showed that the noise affects the speed estimation as we can see from the difference between the actual and the noisy estimates in the figure. In addition, we noticed that the difference between the actual and noise-free estimates is due to the change of the crossing cohort size, and this happens only when a new pedestrian joins the cohort. We show in Fig. 13(b) the ECDF after removing the samples where a new pedestrian joins the cohort. As it can be seen in the figure, the difference between the noise-free estimated speed and the actual speed is lower when the cohort size is fixed.

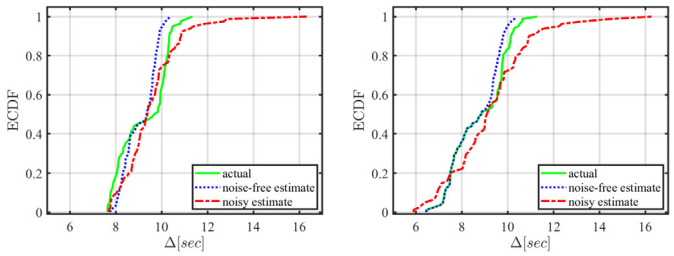

(a) *Dynamic cohort size* (b) *Fixed cohort size*

Fig. 14. ECDF of remaining crossing time.

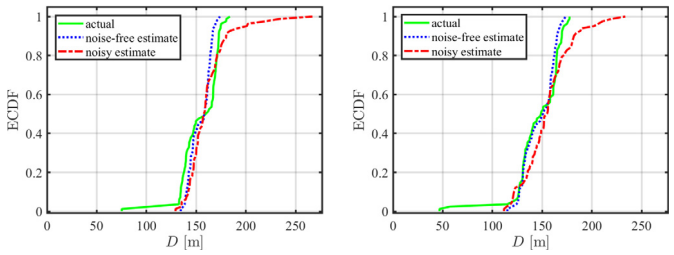

(a) *Dynamic cohort size* (b) *Fixed cohort size*

Fig. 15. ECDF of propagation distance.

8.3.4. Accuracy of the remaining crossing time

We used the same RMSE formula to measure the accuracy of the remaining crossing time:

$$E_{\Delta} = \sqrt{\frac{\Sigma_{i=1}^{N}(\hat{\Delta}_i - \Delta_i)^2}{N}}$$

where $\hat{\Delta}_i$ and Δ_i are, respectively, the actual and estimated remaining time to cross for each pedestrian. The results show that ADOPT RMSE in crossing time estimation E_{Δ} was less than 1 sec in noise-free mode while it has higher error in the noisy mode. Fig. 14(a) shows the ECDF of the average crossing time for each pedestrian in the street. We calculated the actual remaining crossing time based on the actual speed retrieved from SUMO. As the noise affects the speed, it also affects the remaining crossing time as we show in the figure. We noticed also that the difference between the actual and noise-free estimation is due to the change of the crossing cohort size, and this happens only the first time a new signal is detected in the crossing cohort. We show in Fig. 14(b) the ECDF after removing the samples where a new pedestrian joins the cohort. As it can be seen from the figure, the difference between the noise-free estimate and the actual time to cross is lower.

8.3.5. Accuracy of Safety Zone size

The RMSE of estimating the Safety Zone size, which is determined by the propagation distance $D(t)$, for each pedestrian is calculated as follows:

$$E_{D} = \sqrt{\frac{\Sigma_{i=1}^{N}(\hat{D}_i - D_i)^2}{N}}$$

where $\hat{D}_i$ and D_i are, respectively, the actual and estimated propagation distances. $\hat{D}_i$ is calculated based on the actual remaining time to cross $\hat{\Delta}_i$. Fig. 15 shows the ECDF for the propagation distance estimation averaged for each pedestrian in the dynamic and fixed cohort sizes. We noticed that the difference between the actual and the noise-free estimate is less in the fixed cohort size. The difference between them increases based on the error of Δ estimation.

To justify the difference between the actual and estimated propagation distance, we measured the relative error of estimating Δ and D in noise-free mode for fixed size cohort compared to their actual values where the $relative\ error = actual\ value - estimated\ value$. The results showed that there is a high correlation between the relative error of estimating Δ and D as we show in Fig. 16. The figure also shows that the majority of Δ errors are less than 3 seconds and cause about additional 40 meters of D. We see a high error in D since each ± 1 second of error in Δ is multiplied by the car's speed and the added r, so this second produces about ± 15 meters of D error. If the error is positive then ADOPT estimates a larger safety zone and the pedestrian is safe. Indeed, the risk may increase if the estimation is less than needed.

In conclusion, the ADOPT classification accuracy depends on the amount of RSS noise that affects the $c(\Gamma)$ values near the edge of the sidewalk. For localization, the accuracy of ADOPT depends on the RSS noise and the distance of the pedestrian from the transceiver receiving the strongest signals. ADOPT accuracy in estimating the speed, remaining crossing time and Safety Zone size depends on the noise and changes in cohort size.

8.3.6. Evaluation of occluded pedestrian protection

To evaluate the performance of ADOPT as an end-to-end system to protect occluded crossing pedestrians, we calculated the speed of the approaching car upon reaching the pedestrian crossing area. We assumed that the driver or the automated vehicle react to the "Caution" message promptly upon receiving it from the ADOPT app running in the car.

Referring to Fig. 17, the approaching cars generated in SUMO adopt the new speed v_{safe} upon receiving the "Caution" messages as they approach the crossing pedestrians. We observed and aggregated the speeds at every 13-meters of car-to-pedestrians distances. As it can be seen also in the figure, the cars start maintaining their safe speeds gradually while they are approaching the crossing pedestrians which allows a smooth speed reduction without the need for a sudden stop.

To compare the speed reduction caused by ADOPT with the speed of cars without ADOPT, we plotted their cruising speeds $v_{cruising}$ from SUMO in the same figure. We called it $v_{cruising}$ since SUMO cars do not maintain a fixed speed while moving, and also each car has its own speed random distribution with a determined maximum speed equal to the street's speed limit v_{max}.

In the following, we show some examples from the simulation of approaching cars receiving ADOPT "Caution" message and changing their speed accordingly. In Fig. 18(a), the approaching car with speed v_{max} receives a "Caution" message at location C and time $s1$ for a pedestrian crossing at location $L1$. The car reduces its speed to v_{safe} as a response to the alert message. We noticed that the car may intersect slightly before $(L1, e1)$ due to the error in estimating d and the crossing time Δ. In another example Fig. 18(b), the car receives another "Caution" message at location C' as a new pedestrian joins the cohort from the same location of L, and finishes crossing at $e2 > e1$. In this case, the car finds that the new speed (denoted by $v_{safe'}$) is lower than v_{safe}, so it adopts the new speed $v_{safe'}$ to avoid the collision. The expected reaction of the approaching car is to reduce its speed because the crossing time now becomes longer as a new pedestrian joins the cohort.

In a more complex example, cars report pedestrians at different locations $L1$ and $L2$ as in Fig. 18(c). When the car receives a new "Caution" message at time $s2$ and location C', it calculates the new speed and finds that it is less than its current speed because $L2$ is closer than $L1$. Thus, it adopts the new speed $v_{safe'}$ until the pedestrian finish crossing.

In conclusion, approaching cars were able to maintain low speeds to avoid collision with the occluded crossing pedestrian accurately and in a timely manner based on the "Caution" messages

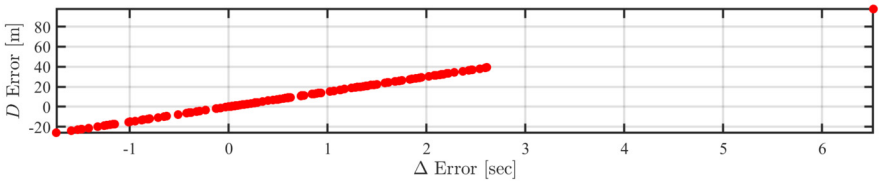

Fig. 16. Correlation between the estimation error of D and Δ.

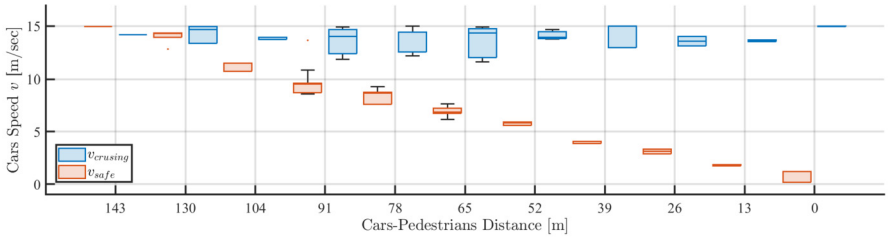

Fig. 17. All approaching cars maintained safe speeds upon receiving the "Caution" message from ADOPT while they keep their cruising speeds without ADOPT "Caution" messages.

received from ADOPT. This proves that ADOPT works end-to-end to effectively protect crossing pedestrians.

9. Concluding remarks and future work

The common philosophy of all the pedestrian detection approaches of which we are aware is that this task should be undertaken by the moving cars themselves. In sharp departure from this philosophy, we proposed to employ cars parked along the sidewalk to detect and protect crossing pedestrians.

In support of this goal, we have proposed ADOPT: a system for Alerting Drivers to Occluded Pedestrian Traffic. ADOPT lays the theoretical foundations of a system that uses the on-board resources of parked cars to:

- Detect the presence of a group of crossing pedestrians – a crossing cohort;
- Predict the time the last member of the cohort takes to cross the street;
- Send alert messages to those approaching cars that may reach the crossing area while pedestrians are still in the street;
- Show how approaching cars can adjust their speed to avoid crashing into crossing pedestrians.

Importantly, in ADOPT communications occur over very short distances and at very low power. Our extensive simulations using SUMO-generated pedestrian and car traffic, have shown the effectiveness of ADOPT in detecting and protecting crossing pedestrians.

In spite of this, there are a number of topics that need more work:

- First, it is important to consider cars that are not parked parallel to the sidewalk, e.g., cars that are parked at an angle;
- Second, we will investigate the problem of information overload. The problem arises when the (human) driver of an approaching car is alerted to the presence of various crossing cohorts. We are planning to design an app that minimized the information overload and, consequently, driver distraction;
- Third, it is of interest to optimize the process of disseminating alert messages as a function of the residual crossing time. In the current version of the paper "All clear" messages informing approaching cars that the cohort has finished crossing are not used. Incorporating them into ADOPT is targeted for future work;
- Fourth, it is important to investigate the additional fuel consumption, if any, attributable to ADOPT. We conjecture that ADOPT does not result in increased fuel consumption. Along the same line of thought, it is important to investigate the effect of ADOPT on pollution and gas emissions;
- Fifth, in this paper we have assumed that the sidewalk is modeled by a straight line. In many cases, however, the geometry of the street is vastly different, with curvilinear sidewalks prevailing. Naturally, this general sidewalk geometry presents more opportunities for occluded pedestrian traffic. It is important to extend ADOPT to handle gracefully this general scenario;
- Last, but certainly not least, security and privacy are very important and are getting active attention as discussed in the next subsection.

9.1. Security and privacy in ADOPT

ADOPT involves two types of wireless communications: V2P and V2V. In the following, we discuss the security aspects of our communication types.

- Pedestrian to parked vehicle communications: In the pedestrian detection and localization process, the system reads transmitted signals and makes decisions based solely on the signal strength and not on the identity of the pedestrians. These decisions are based on anonymous received signal strengths that do not require unique identifiers. Also, ADOPT detects and localizes pedestrians in short-range communications that do not require transmitting the pedestrians' private data. With the proposed mechanism of pedestrian localization, ADOPT preserves pedestrians' privacy and security. In spite of this, we may consider a potential attack that may be mounted against ADOPT such as a Denial of Service (DoS) attack. In this attack, a group of pedestrians may stomp their feet on the ground to activate the system. Our approach to pedestrian classification can distinguish if the signal is coming from the sidewalk or the street. If this group of people is generating signals from the street, they are at risk and the system should notify approaching cars regardless of their intent.
- Parked vehicle to approaching vehicle communication: This type of communication involves the known security threats in V2V communications [62]. However, the short-range communication used in our system should allow the use of frequency hopping [63] to prevent attackers from sniffing or injecting

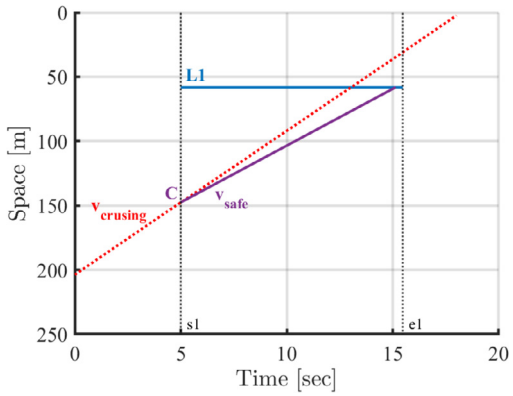

(a) *One pedestrian crossing the street.*

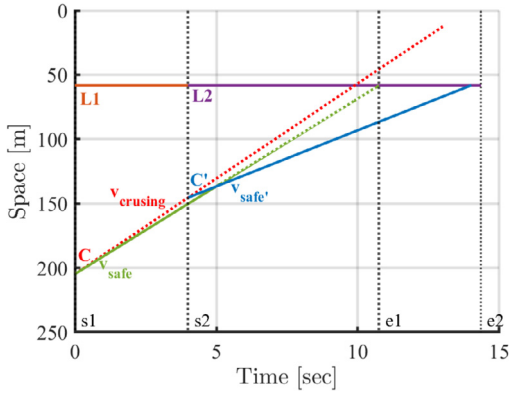

(b) *Multiple pedestrians crossing the street at the same location*

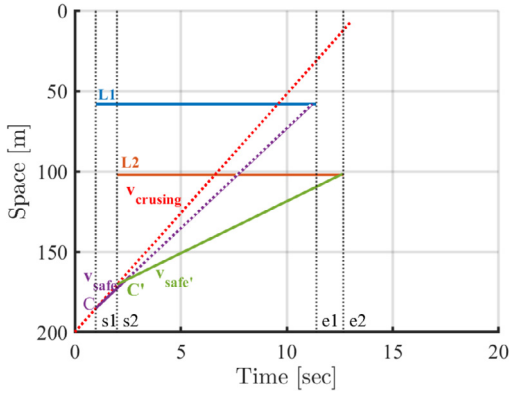

(c) *Multiple pedestrians are crossing the street at different locations.*

Fig. 18. Moving vehicle reduces its speed upon receiving "Caution" message from ADOPT in many cases.

fake information into V2V network. Moreover, short-range V2V communications have their security advantages [10] that are not present in long-range V2V communications. It is of great interest to develop security primitive that leverage the type of short-rage communications that are used throughout the system [64].

Declaration of competing interest

The authors declare the following financial interests/personal relationships which may be considered as potential competing interests: Abrar Alali reports financial support was provided by Saudi Electronic University. Stephan Olariu reports financial support was provided by National Science Foundation, grant number CNS-1951789. Shubham Jain reports financial support was provided by National Science Foundation, grant number CNS-2106594.

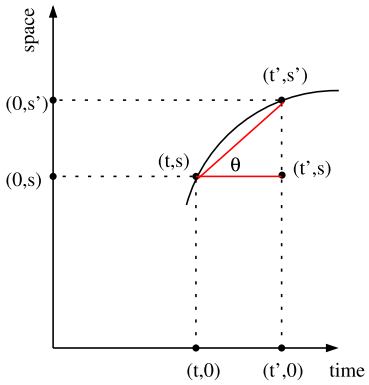

Fig. 19. Illustrating the time-space diagram.

Data availability

Data will be made available on request.

Appendix A

A.1. The time-space diagram

One of the basic tools in the tool-box of traffic engineers is the *time-space diagram* that allows one to plot the trajectories of vehicles as curves in a Cartesian plane with axes labeled "time" and "space". Referring to Fig. 19, the vehicle's coordinates at time t are (t, s). The projection of this point on the vertical axis, $(0, s)$, indicates the position, at time t, of a vehicle that moves along the space axis North-bound (i.e. from bottom to top).

Assume that the same vehicle has continued moving along its trajectory in such a way that at time t', $(t' > t)$, its coordinates in the time-space coordinate system are (t', s'). Equivalently, in the time interval $[t, t']$, the vehicle has moved along the space axis from location $(0, s)$ to location $(0, s')$.

One of the nice features of the time-space diagram is that it allows one to compute and to *visualize* the average speed of the vehicle. Indeed, referring again to Fig. 19, elementary physics indicate that the average speed, v_{avg}, of the vehicle in the time interval $[t, t']$ is the ratio

$$v_{avg} = \frac{s' - s}{t' - t}. \tag{21}$$

This is the same as the *slope* of the line segment connecting the points of coordinates (t, s) and (t', s'). Equivalently, the average speed v_{avg} is $\tan(\theta)$, where θ is the angle determined by the line segment connecting the points of coordinates (t, s) and (t', s') and the positive direction of the time axis.

Finally, it is not hard to see that the *instantaneous speed* of the vehicle at an arbitrary time τ, $(t \leq \tau \leq t')$ turns out to be the slope of the tangent to the trajectory at time τ. In particular, if the trajectory happens to be a straight line, then the average speed matches the instantaneous speed, as expected.

A.2. Time-space diagram of a crossing cohort

Let us turn our attention to the time-space diagram corresponding to a crossing cohort. Referring to Fig. 20, imagine a crossing cohort at location L that starts crossing the street at time $s1$

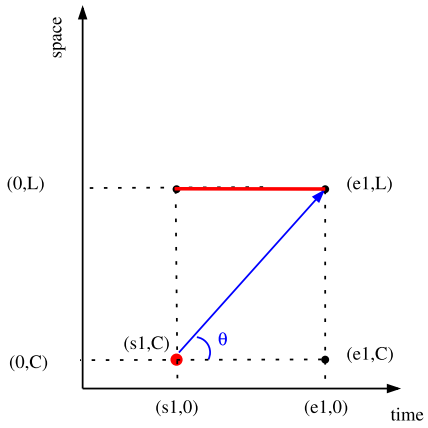

Fig. 20. Illustrating the time-space diagram of a crossing pedestrian.

and clears the street by time $e1$. Since the "space" coordinate of the cohort does not change, the corresponding time-space diagram is captured by a horizontal line segment with endpoints $(s1, L)$ and $(e1, L)$.

Now, consider an approaching car and assume that the coordinates of the car when it receives the "Caution – pedestrian in the street" message are $(s1, C)$. What is the largest average speed that the approaching car should adopt to avoid crashing into the cohort? The answer is simple: the car should not reach the point $(0, L)$ while the crossing is in progress, namely in the time interval $[s1, e1)$. However, the car may reach $(0, L)$ at time $e1$, as by that time the cohort has finished crossing safely. Thus, using (21), the car should adopt the following *safe average speed*:

$$v_{safe} = \min\left\{v_{max}, \frac{L-C}{e1-s1}\right\} \tag{22}$$

where v_{max} is the speed limit on the road considered. Assuming that $\frac{L-C}{e1-s1} \leq v_{max}$, this safe speed is visualized in Fig. 20 as the slope of the blue segment connecting the points $(s1, C)$ and $(e1, L)$.

References

[1] G.H.S.A. Pedestrian, Traffic fatalities by state: 2021 preliminary data, https://www.ghsa.org/resources/Pedestrians22, June 2021.

[2] L. Yue, M. Abdel-Aty, Y. Wu, O. Zheng, J. Yuan, In-depth approach for identifying crash causation patterns and its implications for pedestrian crash prevention, J. Saf. Res. 73 (2020) 119–132.

[3] S. El Hamdani, N. Benamar, M. Younis, Pedestrian support in intelligent transportation systems: challenges, solutions and open issues, Transp. Res., Part C, Emerg. Technol. 121 (2020) 102856.

[4] I. Mahdinia, A.J. Khattak, A. Mohsena Haque, How effective are pedestrian crash prevention systems in improving pedestrian safety? Harnessing large-scale experimental data, Accid. Anal. Prev. 171 (2022) 106669.

[5] S. Gilroy, E. Jones, M. Glavin, Overcoming occlusion in the automotive environment—a review, IEEE Trans. Intell. Transp. Syst. 22 (1) (2019) 23–35.

[6] C. Ning, L. Menglu, Y. Hao, S. Xueping, L. Yunhong, Survey of pedestrian detection with occlusion, Complex Intell. Syst. 7 (1) (2021) 577–587.

[7] S. Zhang, R. Benenson, M. Omran, J. Hosang, B. Schiele, How far are we from solving pedestrian detection?, in: Proceedings of the iEEE Conference on Computer Vision and Pattern Recognition, 2016, pp. 1259–1267.

[8] P. Sun, A. Boukerche, Challenges and potential solutions for designing a practical pedestrian detection framework for supporting autonomous driving, in: Proc. 18th ACM Symposium on Mobility Management and Wireless Access (MobiWac'20), 2020, pp. 75–82.

[9] T. Combs, L. Sandt, M. Clamann, N. McDonald, Automated vehicles and pedestrian safety: exploring the promise and limits of pedestrian detection, Am. J. Prev. Med. 56 (1) (2019) 1–7.

[10] D.B. Rawat, B.B. Bista, G. Yan, S. Olariu, Vehicle-to-Vehicle connectivity and communication framework for vehicular Ad-Hoc networks, in: 2014 8-th International Conference on Complex, Intelligent and Software Intensive Systems, 2014, pp. 44–49.

[11] P. Sewalkar, J. Seitz, Vehicle-to-Pedestrian communication for vulnerable road users: survey, design considerations, and challenges, Sensors 19 (2) (Jan. 2019).

[12] O. Grembek, A. Kurzhanskiy, A. Medury, P. Varaiya, M. Yu, Making intersections safer with I2V communication, Transp. Res., Part C, Emerg. Technol. 102 (2019) 396–410.

[13] S. Zhang, M. Abdel-Aty, Y. Wu, O. Zheng, Pedestrian crossing intention prediction at Red-Light using pose estimation, IEEE Trans. Intell. Transp. Syst. (2021) 1–9.

[14] H.O. Tezcan, M. Elmorssy, G. Aksoy, Pedestrian crossing behavior at midblock crosswalks, J. Saf. Res. 71 (2019) 49–57.

[15] X. Li, Y.-J. Wu, Real-time estimation of pedestrian volume at button-activated midblock crosswalks using traffic controller event-based data, Transp. Res., Part C, Emerg. Technol. 122 (2021) 102876.

[16] C. Zhang, B. Zhou, G. Chen, F. Chen, Quantitative analysis of pedestrian safety at uncontrolled multi-lane mid-block crosswalks in China, Accid. Anal. Prev. 108 (2017) 19–26.

[17] D. Eckhoff, C. Sommer, R. German, F. Dressler, Cooperative awareness at low vehicle densities: how parked cars can help see through buildings, in: 2011 IEEE Global Telecommunications Conference - GLOBECOM 2011, 2011, pp. 1–6.

[18] C. Sommer, D. Eckhoff, F. Dressler, IVC in cities: signal attenuation by buildings and how parked cars can improve the situation, IEEE Trans. Mob. Comput. 13 (8) (2014) 1733–1745.

[19] S.W. Loke, Cooperative automated vehicles: a review of opportunities and challenges in socially intelligent vehicles beyond networking, IEEE Trans. Intell. Veh. 4 (4) (2019) 509–518.

[20] R. Yee, E. Chan, B. Cheng, G. Bansal, Collaborative perception for automated vehicles leveraging Vehicle-to-Vehicle communications, in: 2018 IEEE Intelligent Vehicles Symposium (IV), 2018, pp. 1099–1106.

[21] X. Wu, S. Subramanian, R. Guha, R.G. White, J. Li, K.W. Lu, A. Bucceri, T. Zhang, Vehicular communications using DSRC: challenges, enhancements, and evolution, IEEE J. Sel. Areas Commun. 31 (9) (2013) 399–408.

[22] I. Standard, Road vehicles–Controller Area Network (CAN) – part 1: data link layer and physical signalling, ISO 11898 (2003) 1.

[23] R.D. Brehar, M.P. Muresan, T. Marița, C.-C. Vancea, M. Negru, S. Nedevschi, Pedestrian Street-Cross action recognition in monocular far infrared sequences, IEEE Access 9 (2021) 74302–74324.

[24] G. De Nicolao, A. Ferrara, L. Giacomini, Onboard Sensor-Based collision risk assessment to improve pedestrians' safety, IEEE Trans. Veh. Technol. 56 (5) (2007) 2405–2413.

[25] Z. Chen, X. Huang, Pedestrian detection for autonomous vehicle using Multi-Spectral cameras, IEEE Trans. Intell. Veh. 4 (2) (2019) 211–219.

[26] S. Zhang, J. Yang, B. Schiele, Occluded pedestrian detection through guided attention in cnns, in: Proceedings of the IEEE Conference on Computer Vision and Pattern Recognition, 2018, pp. 6995–7003.

[27] C. Zhou, M. Yang, J. Yuan, Discriminative feature transformation for occluded pedestrian detection, in: Proceedings of the IEEE/CVF International Conference on Computer Vision, 2019, pp. 9557–9566.

[28] Y. He, C. Zhu, X.-C. Yin, Occluded pedestrian detection via Distribution-Based Mutual-Supervised feature learning, IEEE Trans. Intell. Transp. Syst. (2021) 1–16.

[29] Y. Pang, J. Xie, M.H. Khan, R.M. Anwer, F.S. Khan, L. Shao, Mask-guided attention network for occluded pedestrian detection, in: Proceedings of the IEEE/CVF International Conference on Computer Vision, 2019, pp. 4967–4975.

[30] A. Palffy, J.F.P. Kooij, D.M. Gavrila, Occlusion aware sensor fusion for early crossing pedestrian detection, in: 2019 IEEE Intelligent Vehicles Symposium (IV), 2019, pp. 1768–1774.

[31] S.K. Kwon, E. Hyun, J.-H. Lee, J. Lee, S.H. Son, A Low-Complexity scheme for partially occluded pedestrian detection using LIDAR-RADAR sensor fusion, in: 2016 IEEE 22nd International Conference on Embedded and Real-Time Computing Systems and Applications (RTCSA), 2016, p. 104.

[32] P.-F. Ho, J.-C. Chen, WiSafe: Wi-Fi pedestrian collision avoidance system, IEEE Trans. Veh. Technol. 66 (6) (2017) 4564–4578.

[33] K. Dhondge, S. Song, B.-Y. Choi, H. Park, WiFiHonk: Smartphone-Based beacon stuffed WiFi Car2X-Communication system for vulnerable road user safety, in: 2014 IEEE 79th Vehicular Technology Conference, VTC Spring, 2014, pp. 1–5.

[34] P. Wang, M. Zhou, Z. Ding, A VRU collision warning system with Kalman-Filter-Based positioning accuracy improvement, in: 2021 IEEE International Conference on Information Communication and Software Engineering (ICICSE), 2021, pp. 191–198.

[35] R. Zhang, L. Song, A. Jaiprakash, T. Talty, A. Alanazi, A. Alghafis, A.A. Biyabani, Ozan Tonguz, Using Ultra-Wideband technology in vehicles for infrastructure-free localization, in: 2019 IEEE 5th World Forum on Internet of Things (WF-IoT), 2019, pp. 122–127.

[36] A. Tahmasbi-Sarvestani, H. Nourkhiz Mahjoub, Y.P. Fallah, E. Moradi-Pari, O. Abuchaar, Implementation and evaluation of a cooperative vehicle-to-pedestrian safety application, IEEE Intell. Trans. Syst. Mag. 9 (4) (2017) 62–75.

[37] P. Merdrignac, O. Shagdar, F. Nashashibi, Fusion of perception and V2P communication systems for the safety of vulnerable road users, IEEE Trans. Intell. Transp. Syst. 18 (7) (2017) 1740–1751.

[38] P. Sun, A. Boukerche, A novel Internet-of-Vehicles assisted collaborative low-visible pedestrian detection approach, in: GLOBECOM 2020 - 2020 IEEE Global Communications Conference, 2020, pp. 1–6.
[39] M. Islam, M. Rahman, M. Chowdhury, G. Comert, E.D. Sood, A. Apon, Vision-Based personal safety messages (PSMs) generation for connected vehicles, IEEE Trans. Veh. Technol. 69 (9) (2020) 9402–9416.
[40] A. Ben Khalifa, I. Alouani, M.A. Mahjoub, A. Rivenq, A novel multi-view pedestrian detection database for collaborative intelligent transportation systems, Future Gener. Comput. Syst. 113 (2020) 506–527.
[41] B. Noh, H. Yeo, A novel method of predictive collision risk area estimation for proactive pedestrian accident prevention system in urban surveillance infrastructure, Transp. Res., Part C, Emerg. Technol. 137 (2022) 103570.
[42] T. Larson, A. Wyman, D.S. Hurwitz, M. Dorado, S. Quayle, S. Shetler, Evaluation of dynamic passive pedestrian detection, Transp. Res. Interdiscip. Perspect. 8 (2020) 100268.
[43] J. Zhao, H. Xu, H. Liu, J. Wu, Y. Zheng, D. Wu, Detection and tracking of pedestrians and vehicles using roadside LiDAR sensors, Transp. Res., Part C, Emerg. Technol. 100 (2019) 68–87.
[44] F. Pereira, H. Sampaio, R. Chaves, R. Correia, M. Luís, S. Sargento, M. Jordão, L. Almeida, C. Senna, A.S.R. Oliveira, N. Borges Carvalho, When backscatter communication meets vehicular networks: boosting crosswalk awareness, IEEE Access 8 (2020) 34507–34521.
[45] N. Liu, M. Liu, W. Lou, G. Chen, J. Cao, PVA in VANETs: stopped cars are not silent, in: 2011 Proceedings IEEE INFOCOM, 2011, pp. 431–435.
[46] S. Abdelhamid, H.S. Hassanein, G. Takahara, Vehicle as a resource (vaar), IEEE Netw. 29 (1) (2015) 12–17.
[47] W.M. Griggs, R. Verago, J. Naoum-Sawaya, R.H. Ordóñez-Hurtado, R. Gilmore, R.N. Shorten, Localizing missing entities using parked vehicles: an RFID-Based system, IEEE Int. Things J. 5 (5) (2018) 4018–4030.
[48] J. Zhao, Z. You, A shoe-embedded piezoelectric energy harvester for wearable sensors, Sensors 14 (7) (2014) 12497–12510.
[49] Q. Huang, Y. Mei, W. Wang, Q. Zhang, Toward Battery-Free wearable devices: the synergy between two feet, ACM Trans. Cyber-Phys. Syst. 2 (3) (2018) 1–18.
[50] A. Zanella, Best practice in RSS measurements and ranging, IEEE Commun. Surv. Tutor. 18 (4) (2016) 2662–2686.
[51] T. Stoyanova, F. Kerasiotis, G. Papadopoulos, Rss-based outdoor localization with wireless sensor networks in practice, in: Technological Breakthroughs in Modern Wireless Sensor Applications, IGI Global, 2015, pp. 225–256.
[52] S. Seneviratne, Y. Hu, T. Nguyen, G. Lan, S. Khalifa, K. Thilakarathna, M. Hassan, A. Seneviratne, A survey of wearable devices and challenges, IEEE Commun. Surv. Tutor. 19 (4) (2017) 2573–2620.
[53] O.K. Tonguz, W. Viriyasitavat, Cars as roadside units: a self-organizing network solution, IEEE Commun. Mag. 51 (12) (2013) 112–120.
[54] A. Sarker, C. Qiu, H. Shen, Connectivity maintenance for Next-Generation decentralized vehicle platoon networks, IEEE/ACM Trans. Netw. 28 (4) (2020) 1449–1462.
[55] M. Aljohani, S. Olariu, A. Alali, S. Jain, A survey of parking solutions for smart cities, IEEE Trans. Intell. Transp. Syst. 23 (8) (2022) 10012–10029.
[56] D. Sam, C. Velanganni, T.E. Evangelin, A vehicle control system using a time synchronized hybrid vanet to reduce road accidents caused by human error, Veh. Commun. 6 (2016) 17–28.
[57] Y.T. Lo, S. Lee, Antenna Handbook: Theory, Applications, and Design, Springer Science & Business Media, 2013.
[58] R. Koppa, Human Factors, 2003.
[59] P.A. Lopez, M. Behrisch, L. Bieker-Walz, J. Erdmann, Y.-P. Flötteröd, R. Hilbrich, L. Lücken, J. Rummel, P. Wagner, E. Wießner, Microscopic traffic simulation using sumo, in: The 21st IEEE International Conference on Intelligent Transportation Systems, 2018, pp. 2575–2582.
[60] W. Bronzi, R. Frank, G. Castignani, T. Engel, Bluetooth low energy for inter-vehicular communications, in: 2014 IEEE Vehicular Networking Conference (VNC), 2014, pp. 215–221.
[61] T. Stoyanova, F. Kerasiotis, K. Efstathiou, G. Papadopoulos, Modeling of the RSS uncertainty for RSS-Based outdoor localization and tracking applications in wireless sensor networks, in: 2010 Fourth International Conference on Sensor Technologies and Applications, ieeexplore.ieee.org, 2010, pp. 45–50.
[62] M. Arif, G. Wang, Z.A. Bhuiyan, T. Wang, J. Chen, A survey on security attacks in VANETs: communication, applications and challenges, Veh. Commun. 19 (2019) 100179.
[63] S. Olariu, A. Wadaa, L. Wilson, M. Eltoweissy, Wireless sensor networks: leveraging the virtual infrastructure, IEEE Netw. 18 (4) (2004) 51–56.
[64] S. El-Tawab, A. Alhafdhi, D. Treeumnuk, D.C. Popescu, S. Olariu, Physical layer aspects of information exchange in the NOTICE architecture, IEEE Intell. Trans. Syst. Mag. 7 (1) (2015) 8–18.
[65] S. Olariu, A survey of vehicular cloud research: trends, applications and challenges, IEEE Trans. Intell. Transp. Syst. 21 (6) (2020) 2648–2663.